ISSN: 2576-6732 (Print)
ISSN: 2576-6724 (Online) Pakistan Journal of Geology (PJG) 2021, VOLUME 5, ISSUE 2

Assessment of Aquifer Vulnerability Using GIS And Multi-Criteria Analysis Within Lead City University, Southwestern Nigeria

Adebo Babatunde A, Jemiriwon Emmanuel Tope and Ilugbo Stephen Olubusola*

Department of Physics, Lead City University Ibadan
*Corresponding Author Email: bussytex4peace44@gmail.com; ilugbo.stephen@lcu.edu.ng

DOI: 10.2478/pjg-2021-0010

Abstract:
This research evaluates aquifer vulnerability within Lead City University Ibadan, Southwestern Nigeria. Multi-Criteria Evaluation Techniques were used for obtaining this aim, with the model which is based on hydraulic conductivity, longitudinal conductance, topsoil resistivity, and thickness of layer overlying aquifer of each sounding point within the entire investigated area for future groundwater development. Electrical Resistivity method using Vertical Electrical Sounding (VES) techniques was obtained across the investigated area using Schlumberger configuration. Twenty (20) VES data points were acquired using Omega Resistivity Meter with maximum current electrode separation (AB/2) of 65 m. The geoelectric results were used to determine second-order parameters and subsequently used to model different geoelectric maps. Three subsurface geoelectric layers were delineated across the investigated area which comprises topsoil, weathered layer, and fresh basement. In this research work, four different aquifer vulnerability parameters; Topsoil Resistivity (TSR), Longitudinal Conductance (LC), Thickness of Layer Overlying Aquifer (TLOA), and Hydraulic Conductivity (HC) were generated and integrated to model the aquifer vulnerability map. It was observed that a small closure at the southwestern and northeastern parts is indicative of a high aquifer vulnerability zone. Moderate aquifer vulnerability zone was observed at the northeastern, southwestern, and western parts of the study area, while low aquifer vulnerability zone was observed at the northern, southern, southeastern, southwestern, central, northeastern, and northwestern parts of the study area. Also, a very low aquifer vulnerability zone was observed in the southwestern part of the study area. The results obtained, indicates that the investigated area is an area of low aquifer vulnerability.

Keywords: Aquifer Vulnerability, Topsoil Resistivity, Hydraulic Conductivity, Longitudinal Conductance, TLOA

1. Introduction

The term groundwater applies to the water of higher than atmospheric pressure contained below the subsurface in saturated fractures, cracks, cavities, and pore, spaces in geologic formations [1-3]. It is distinct from water in the unsaturated zone, which can be below atmospheric pressure and is contained in pores space in the partially air-filled soil region between the subsurface water region and the lithological soil surface [4-6]. The significance of subsurface water and precaution of groundwater contamination is dangerous to efficient water resource management as the solution can be very expensive and often impractical [7, 8]. Consequently, it has become mandatory to carry out a vulnerability assessment to prospect regions with a high risk of contamination [9]. Such vulnerable zones could be cultivated or proper attention should be concentrated on it to prevent pollution and contamination of the subsurface groundwater [10, 11]. Several types of research on vulnerability assessment have illustrated that the protection of porous media on the permeability of the overlying layer to the transportation of contaminants into underlying aquifer regions [12-18]. In the crystalline Basement Complex region, many heeds have been given to the morphology of the vadose zone in delineating the susceptibility of subsurface geological properties underlying aquifers to infiltration of contaminants [19-25]. The flow and extent of contaminant infiltration are controlled majorly with ease by the extent to which the underlying region beneath the location allows penetration of contaminant. Research has revealed that permeable formations allow high infiltration of contaminants while less permeable formation prevents infiltration of contaminants [26-28]. Therefore, the need to understand the subsurface soil properties has become necessary to determine the impact of any overlying contaminant on the underlying aquifer resources. However, Multi-criteria decision analysis is developed for assessing aquifer vulnerability in this study. The vulnerability model was based on integrating some important parameters. Groundwater vulnerability models are evaluated to show regions of high risk for groundwater pollution based on hydrogeologic and human factors. In any model vulnerability map, it is possible to determine specific regions where there is a high risk of contamination putting into account the point of different categories of land cover classes [29]. The principle of multicriteria decision analysis (MCDA) in the context of the analytical hierarchy process (AHP) is deduced as an approach that can yield a prediction model of higher reliability and precision [30]. The proposed technique is applied to geoelectric results and Dar-zarrouk parameters derived from Vertical Electrical Sounding to delineate the aquifer vulnerability model of the investigated area.

2. Site Description and Geology of The Study Area

The area investigated falls within Lead City University and is located along the Toll-gate, Ibadan-Lagos highway, Southwestern Nigeria. It is located at latitudes 7°14’27. 97’’N to 7°14’50.64’’N and longitudes 5°10’5.03”E and 5°10’27.95”E. that is, (805100 to 805900 Northings and 740200 to 740600 Eastings) using the Universal Traverse Marcartor (UTM). The investigated area was characterized by major and minor road. The topography of the area is generally flat and punctuated in some areas by hilly ridges and gentle steeps, with elevations, varying from 320 to 390 m above sea level. The investigation lies within the hard rock terrain and it is underlain by the crystalline basement rocks of Southwestern Nigeria. The major rock type within the study location is Migmatite and banded gneiss and quartzite-quartz schist (Figure 2), which has been reviewed by several workers [31, 32].

.

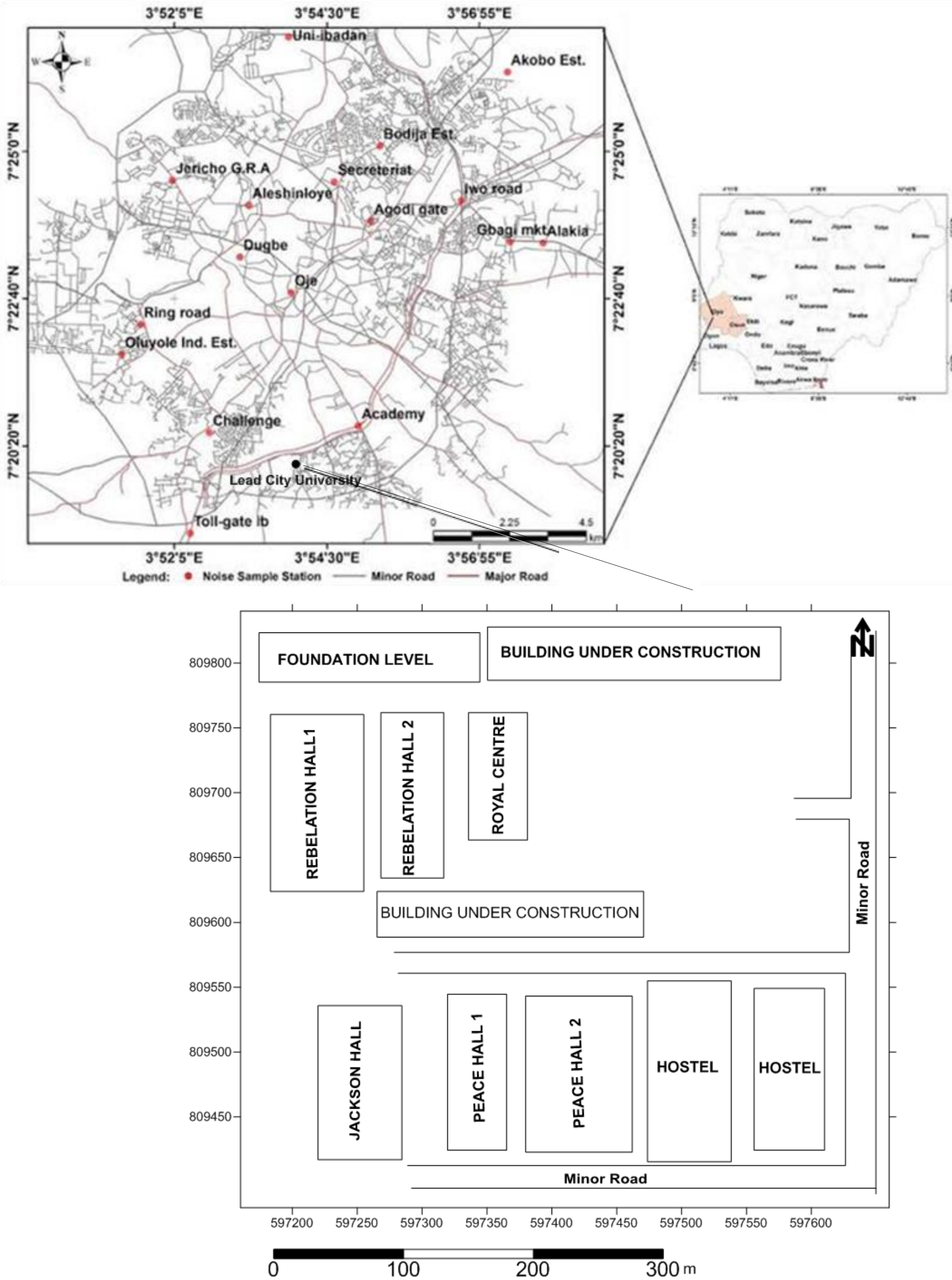

Figure 1: Map of Ibadan Showing the Study Area

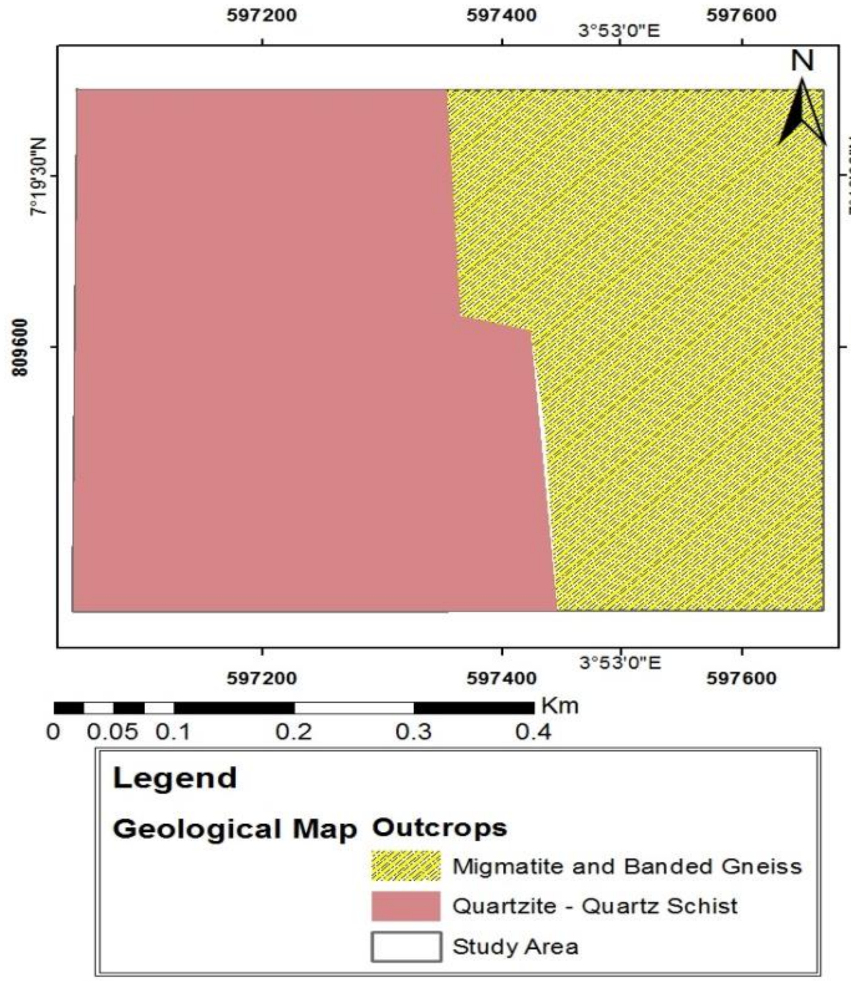

Figure 2: Geological Map of the Study Area [33].

3. Research Methodology

The research includes the generation of the location map and data points in the investigation location, using the GPS and the "ArcGIS 10.5" software; Electrical Resistivity data collection using the Omega Resistivity meter. The Electrical Resistivity method involving Vertical Electrical Sounding (VES) technique utilizing Schlumberger configuration was adopted for these research. Twenty (20) VES points were carried out across the study area with the current electrode spacing (AB/2) of 65 m (Figure 3). The Electrical Resistivity data was processed by plotting apparent resistivity against the electrode spread (AB/2). Processing and interpretation of the VES data were obtained quantitatively to establish the geo-electric/geologic sequence beneath the study area. This was subsequently interpreted quantitatively using the partial curve matching method and computer-assisted1-D forward modeling with WinResist 1.0 version software to determine geoelectric parameters. The geoelectric parameters derived from the interpretation were used to generate the second-order Dar Zarrouk parameters, used to generate appropriate maps. Four factors considered to be of significant influence on aquifer vulnerability were obtained from the geoelectric parameters which are the Topsoil Resistivity (TSR), Longitudinal Conductance (LC), Thickness of Layer Overlying Aquifer (TLOA), Hydraulic Conductivity (HC), and the choice among a set of zones for delineation of aquifer vulnerability was based upon multi-criteria evaluation (MCE) using analytical hierarchy process (AHP) and the final aquifer vulnerability model was produced in ArcGIS environment. Different parameters obtained from geoelectric data have been assigned scores on a numerical scale of 1 to 3 depending upon their significance to aquifer vulnerability. A summation of these values led to the generation of the final weight map.

Mathematically, this can be defined as:

$$AVI = TSR_W TSR_R + LC_W LC_R + TLOA_W TLOA_R + HC_W HC_R \quad (1)$$

Where AVI is Aquifer Vulnerability Index, TSR is Topsoil Resistivity, LC is Longitudinal Conductance, TLOA is Thickness of Layer Overlaying Aquifer and HC is Hydraulic Conductance. The aquifer vulnerability map value, thus derived is given by the equation:

$$AV = \sum WiCVi \text{ ; with } \sum Wi = 1; \quad (2)$$

Where AV is the Aquifer Vulnerability map value, Wi is the probability value of each thematic map, and CVi is the individual capability value to vulnerability.

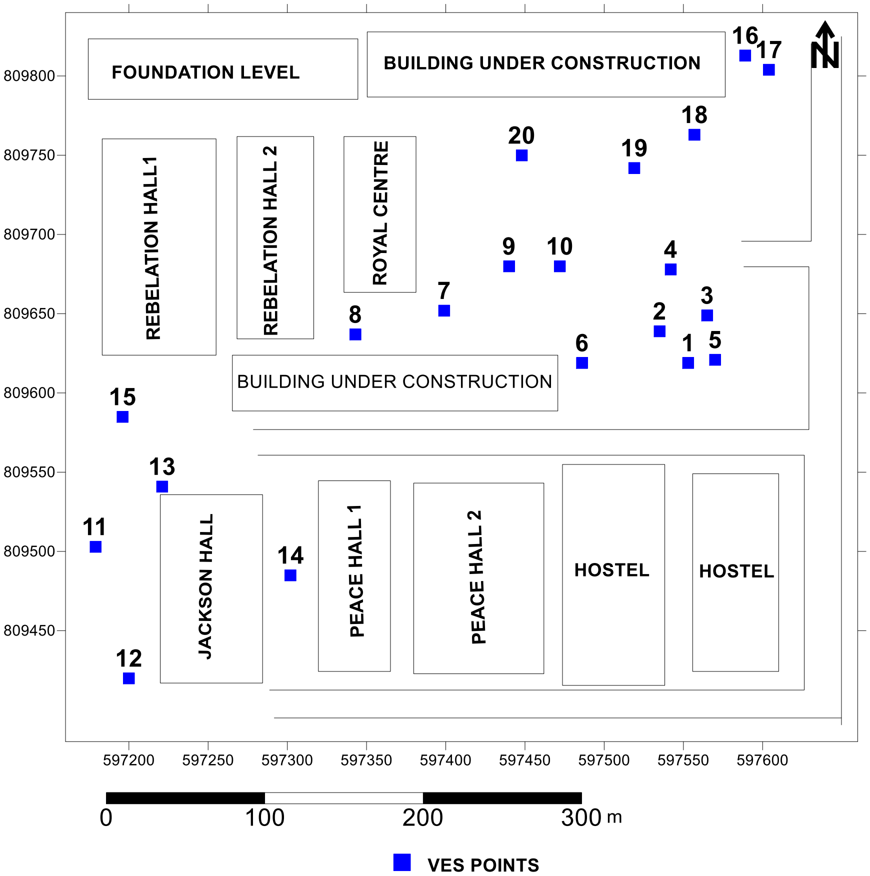

Figure 3: Data Acquisition Map of the Study Area

4. Results and Discussion

4.1. Sounding Curves and Aquifer Types

Two (2) curve types were identified within the study location, these are A and H (Figure 4), with the histogram chart showing the curves type occurrences (Figure 5), where the H curve has the highest percentage (55%) of occurrence.

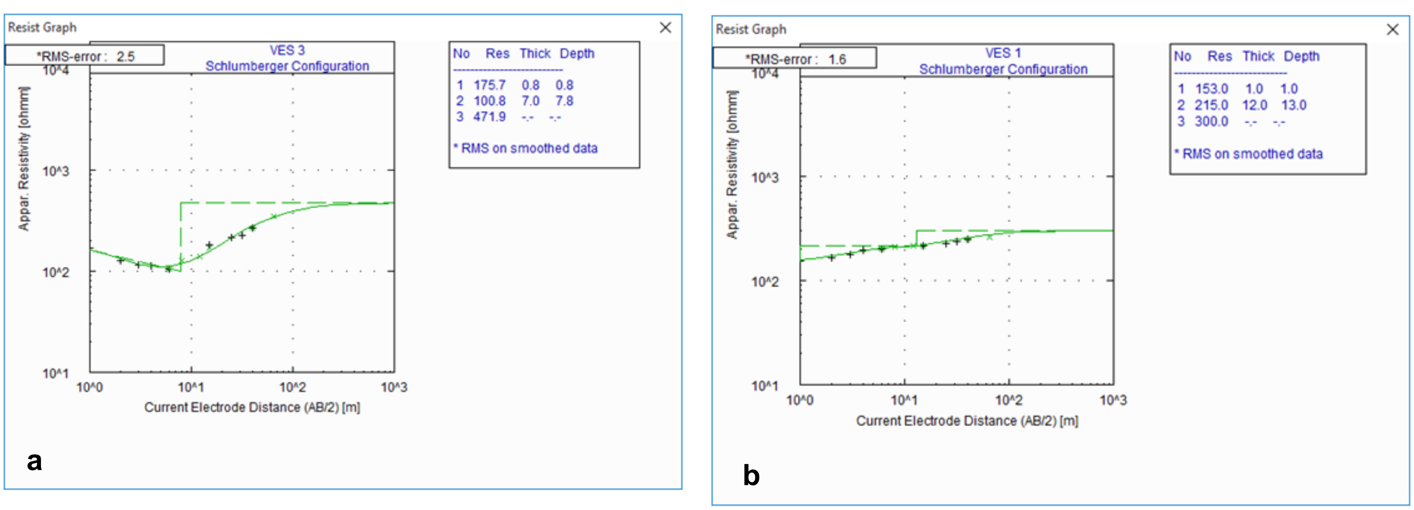

Figure 4: Typical Curve Type (a) H (b) A.

ISSN: 2576-6732 (Print)
ISSN: 2576-6724 (Online) Pakistan Journal of Geology (PJG) 2021, VOLUME 5, ISSUE 2

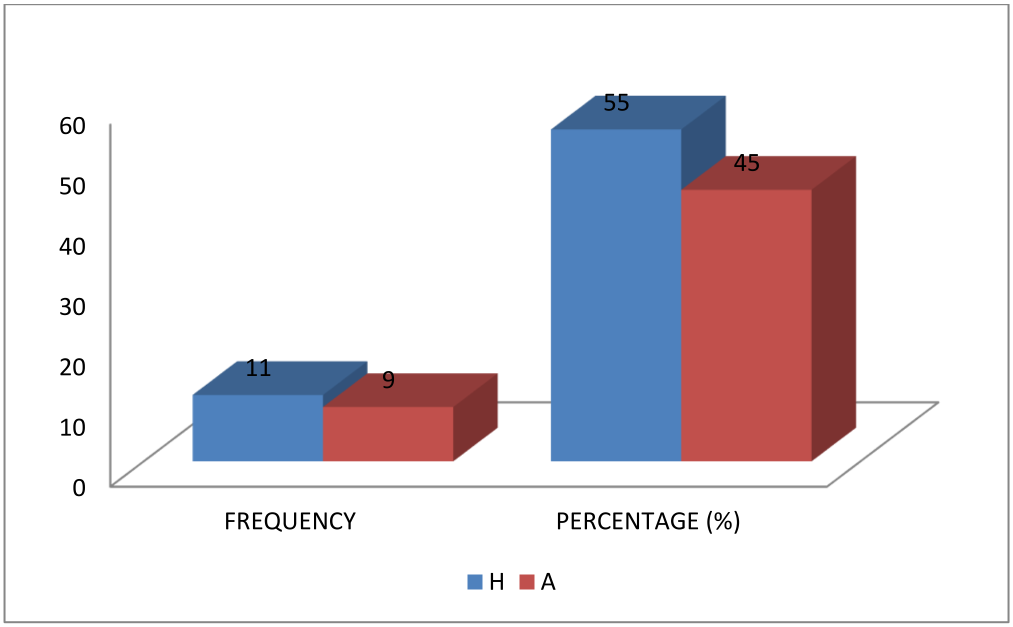

Figure 5: Curve Type Distribution of the Study Area

4.2. Geoelectric Section

To understand the nature of the subsurface rock underlying the investigated area, and a detailed description of the lateral and vertical variation in resistivity, topography, and thickness of the subsurface lithologies, the obtained interpretation results of the Vertical Electrical Sounding (VES) was used to generate four (4) geoelectric sections across the investigated area, approximately SW-NE (Figure 6), N-E (Figure 7), NW-SE (Figure 8), and N-S (Figure 9) directions. Three subsurface geoelectric layers were delineated namely: the topsoil, weathered layer, and fresh basement. The first layer constitutes the topsoil which comprises clay, clayey sand, sandy clay, and sand with layer resistivity ranging from 62 to 226 Ωm with layer thickness varies from 0.7 to 1.7 m. The weathered layer has a resistivity value that ranges from 17 to 311 Ωm with layer thickness varying from 3.4 to 24.1 m, while the last layer is the fresh basement which is characterized by high resistivity values ranging from 429 to 2708 Ωm. The fresh basement is made up of highly resistive crystalline rock. The rocks in this region are not a water-bearing zone due to no permeability, Depth to fresh rocks ranges between 4.9 to 10.4 m.

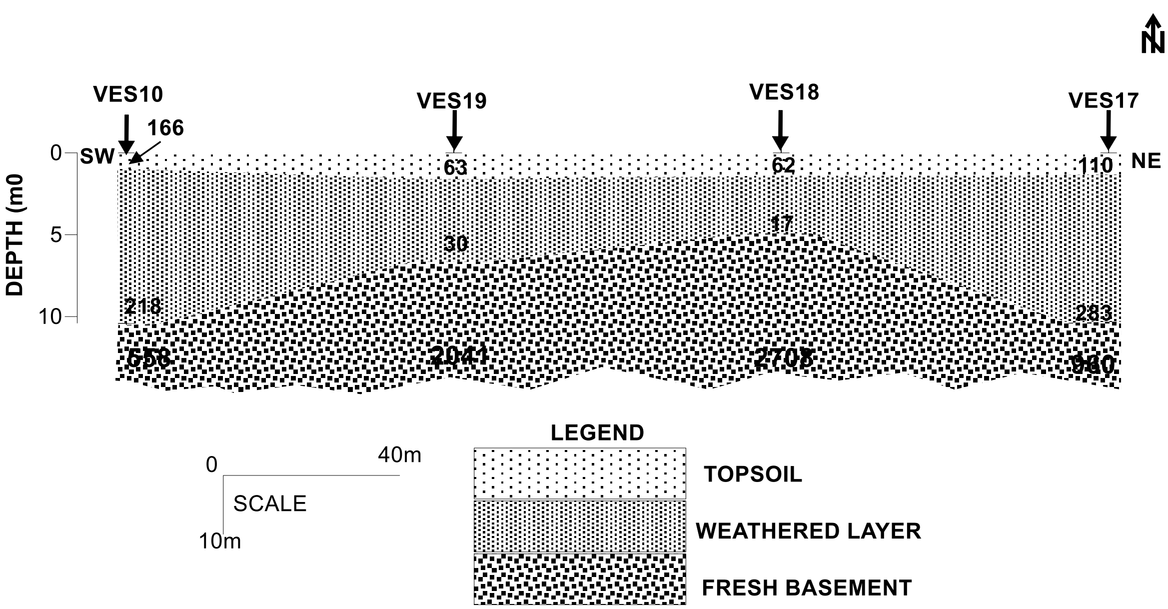

Figure 6: Geoelectric Section along SW – NE Direction

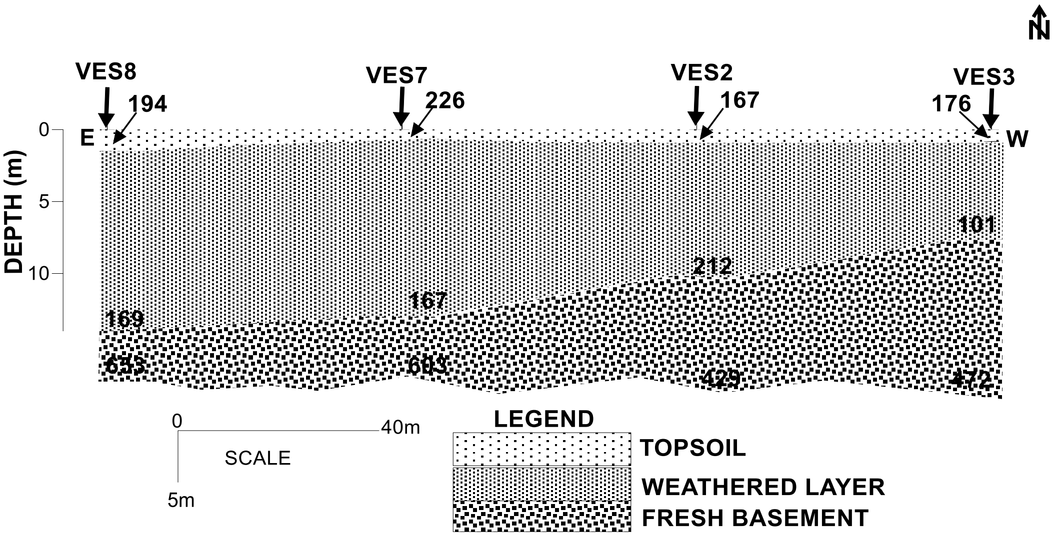

Figure 7: Geoelectric Section along W – E Direction

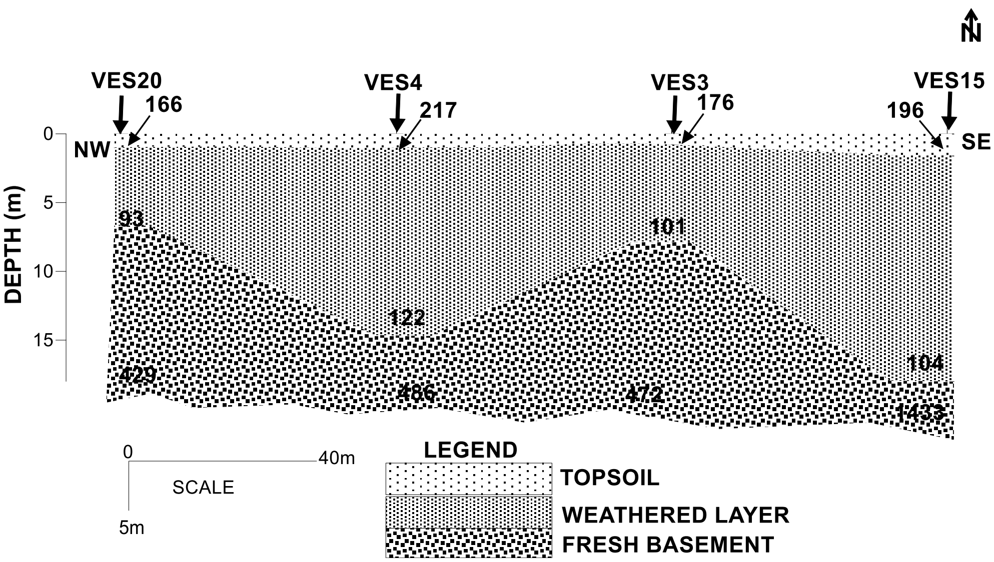

Figure 8: Geoelectric Section along NW – SE Direction

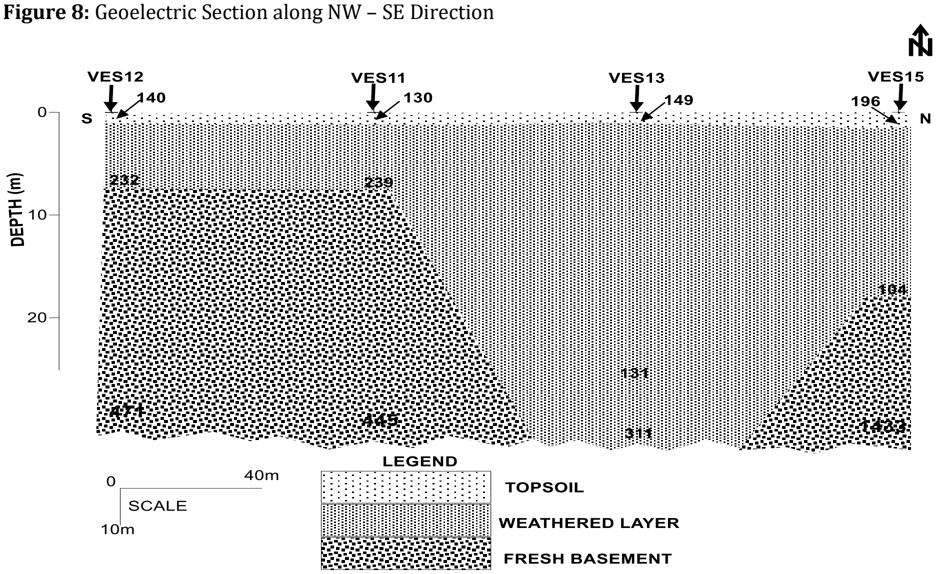

Figure 9: Geoelectric Section along N – S Direction

4.3. Geoelectric Maps

4.3.1. Aquifer Resistivity

The aquifer resistivity model displays relatively low resistivity with values ranging from 17 to 282 Ωm. Area of high aquifer resistivity at the northeastern, southwestern, and small closure at the northeastern parts while northern, northeastern, northwestern, southwestern, and small closure that the southeastern and southwestern parts indicative of moderate aquifer resistivity. Low aquifer resistivities are found at the southern, southeastern, southwestern, northwestern, and central areas of the investigated region which simply shows that the entire area is generally low in terms of aquifer resistivity (Figure 10).

4.3.2. Aquifer Thickness

The aquifer thickness model developed has a value ranging from 3.4 to 25.7 m. the Northern, northeastern, and southeastern indicative of low aquifer thickness while northwestern, central, southwestern, southeastern, and a small closure at northeastern show moderate aquifer thickness. High aquifer thickness was observed in western, southwestern, and southern parts of the investigated area (Figure 11). The region showing moderate to high aquifer resistivity with moderate to high aquifer thickness has a better prospect for groundwater development.

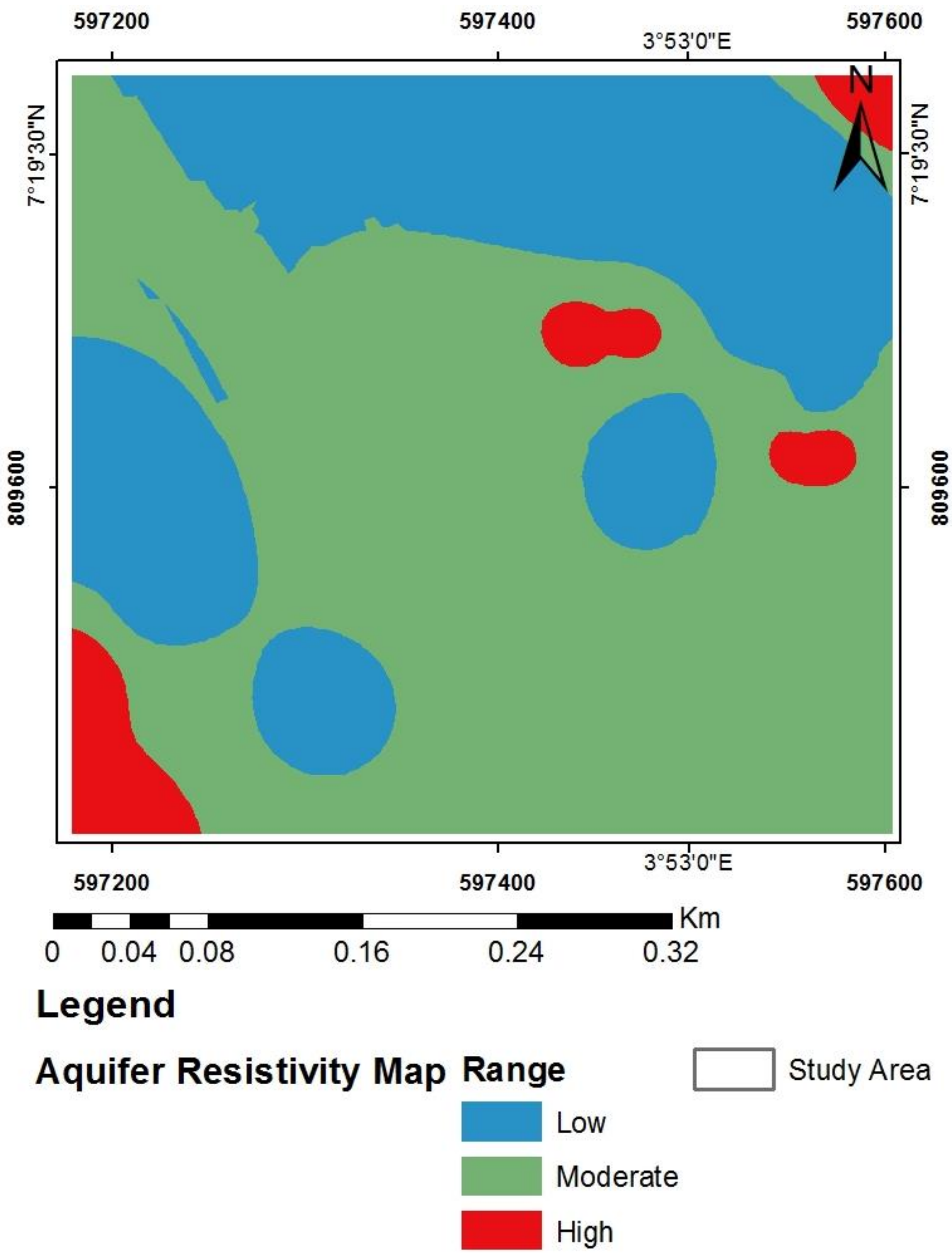

Figure 10: Aquifer Resistivity Map of the Study Area

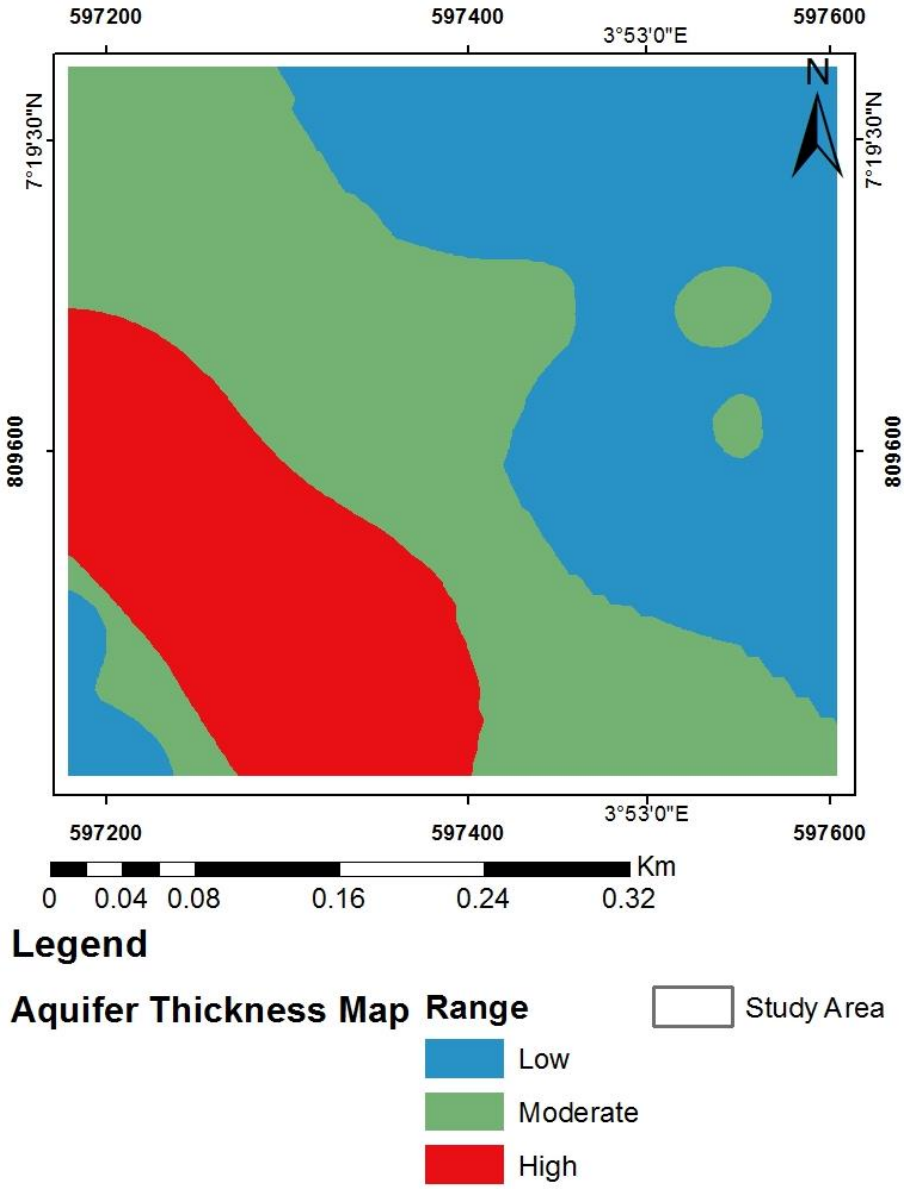

Figure 11: Aquifer Thickness Map of the Study Area.

4.3.3. Overburden thickness map

The overburden thickness map of the investigated area includes the combination of topsoil, the weathered layer, and the fractured basement. The generated depths to the fresh basement under lying the VES points were used to model the overburden thickness map (Figure 12). The overburden thickness varies from 4.9 to 25.7 m. The model displays regions of high overburden (above 19.6 m) in the western, southwestern, and southern parts which favours the groundwater resources in the area most especially when underlain by a weathered basement. The area of high overburden thickness in the southwestern part is surrounded by regions of low overburden thickness (less than 19.6m).

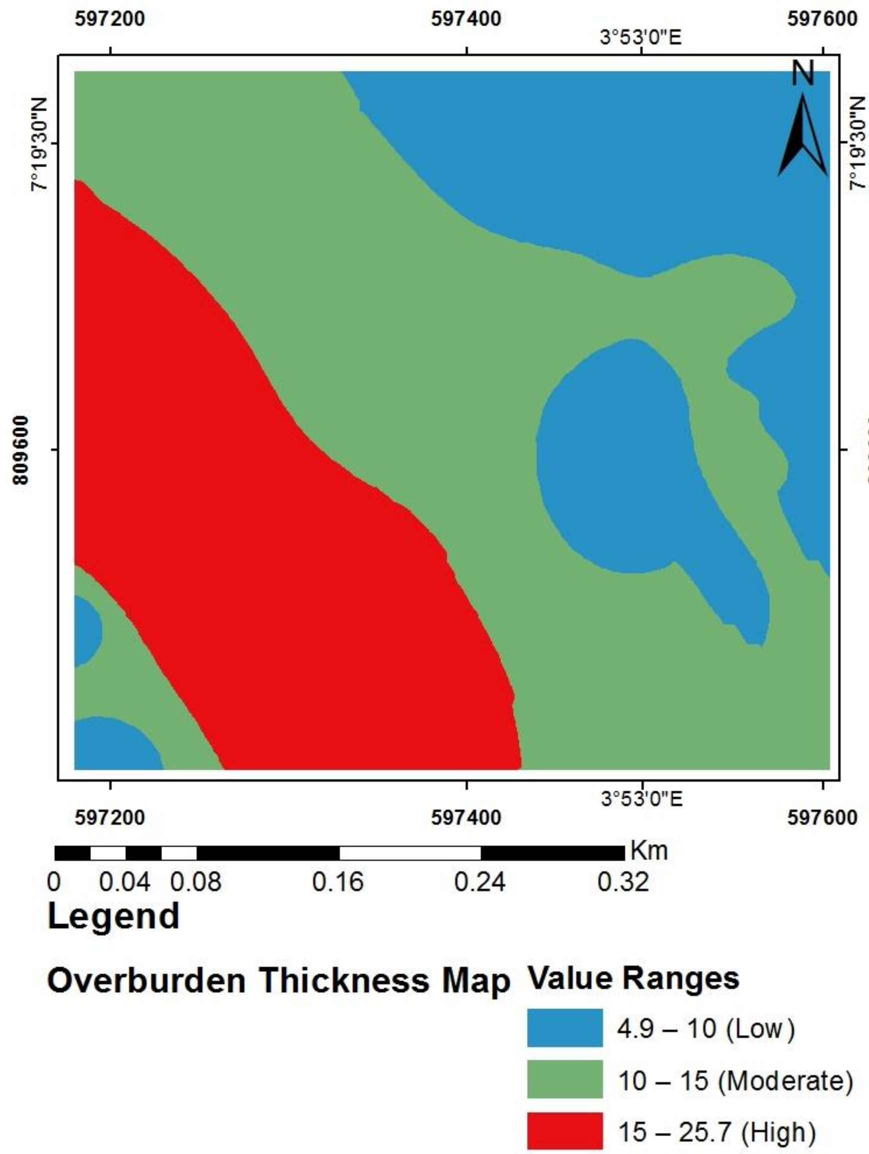

Figure 12: Overburden thickness map

4.3.4. Topsoil Resistivity Map of the Study Area

The topsoil resistivity map (Figure 13) generated displays topsoil resistivity which varies from 61 to 317 Ωm. Area of high topsoil resistivity is found at eastern and small closure at the central and northeastern parts shows that it is highly susceptible to pollution due to the presence of high porosity and permeability of sand presence within these layers while northern, northeastern, northwestern, southwestern, southern, eastern, and western parts indicative of moderate topsoil resistivity shows that it is moderately susceptible to pollution due to the presence of high porosity and little permeability of clayey sand and sandy clay presence. Low topsoil resistivities are found at the northeastern and southwestern parts of the study area which show that this area has low susceptibility to pollution due to the presence of high porosity and low permeability of clay presence within these layers

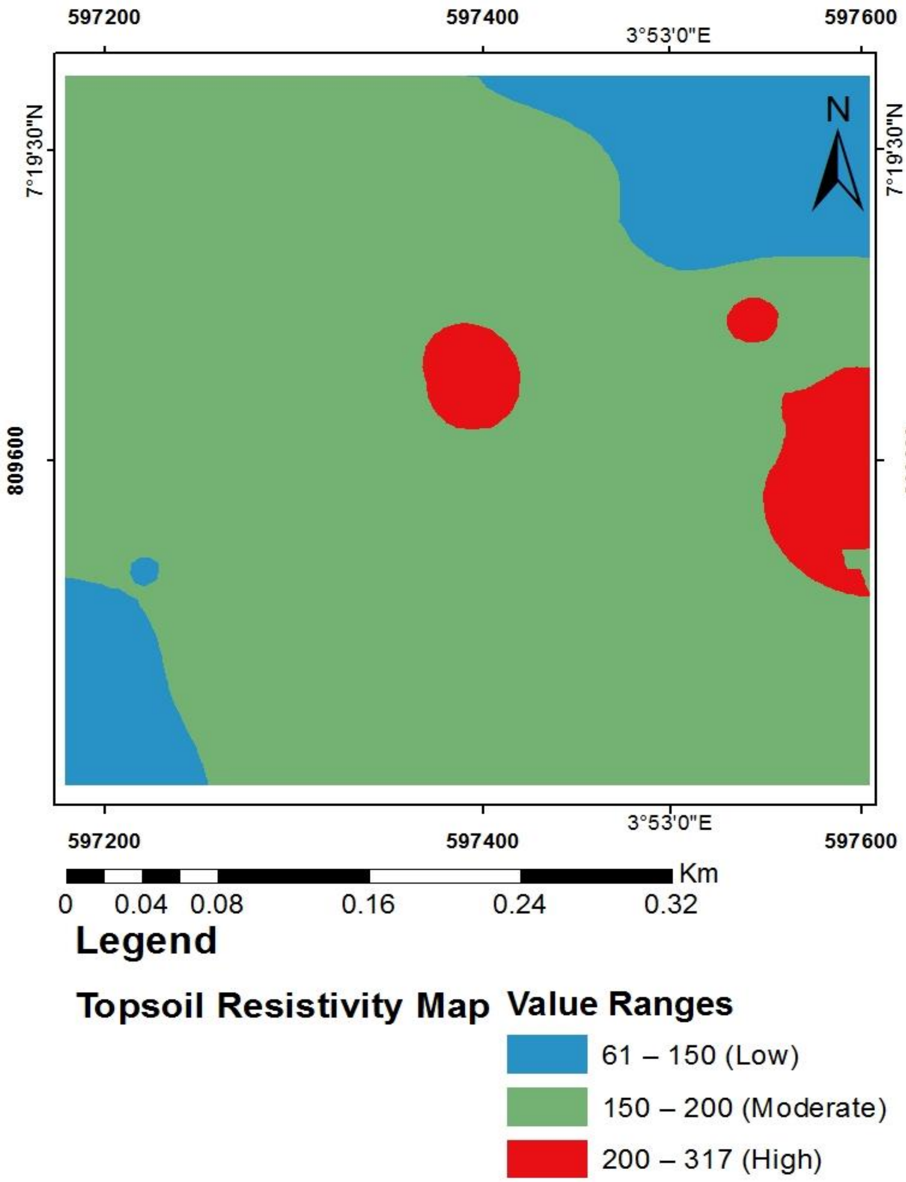

Figure 13: Topsoil Resistivity Map of the Study Area

4.3.5. Thickness of Layer Overlying Aquifer Map of the Study Area

The thickness of the layer overlying the aquifer map (Figure 14) generated shows that the thickness of layer overlying aquifer has values ranging from 0.7 to 1.7 m. Area of the high thickness of layer overlying aquifer is found at northeastern and western parts, while northern, northeastern, northwestern, southwestern, southern, eastern and western parts indicative of the moderate thickness of layer overlying aquifer which shows that the entire area serves as a protective capacity for the aquifer from been contaminated with a small closure of low thickness of layer overlying aquifer found at the northeastern part of the study area.

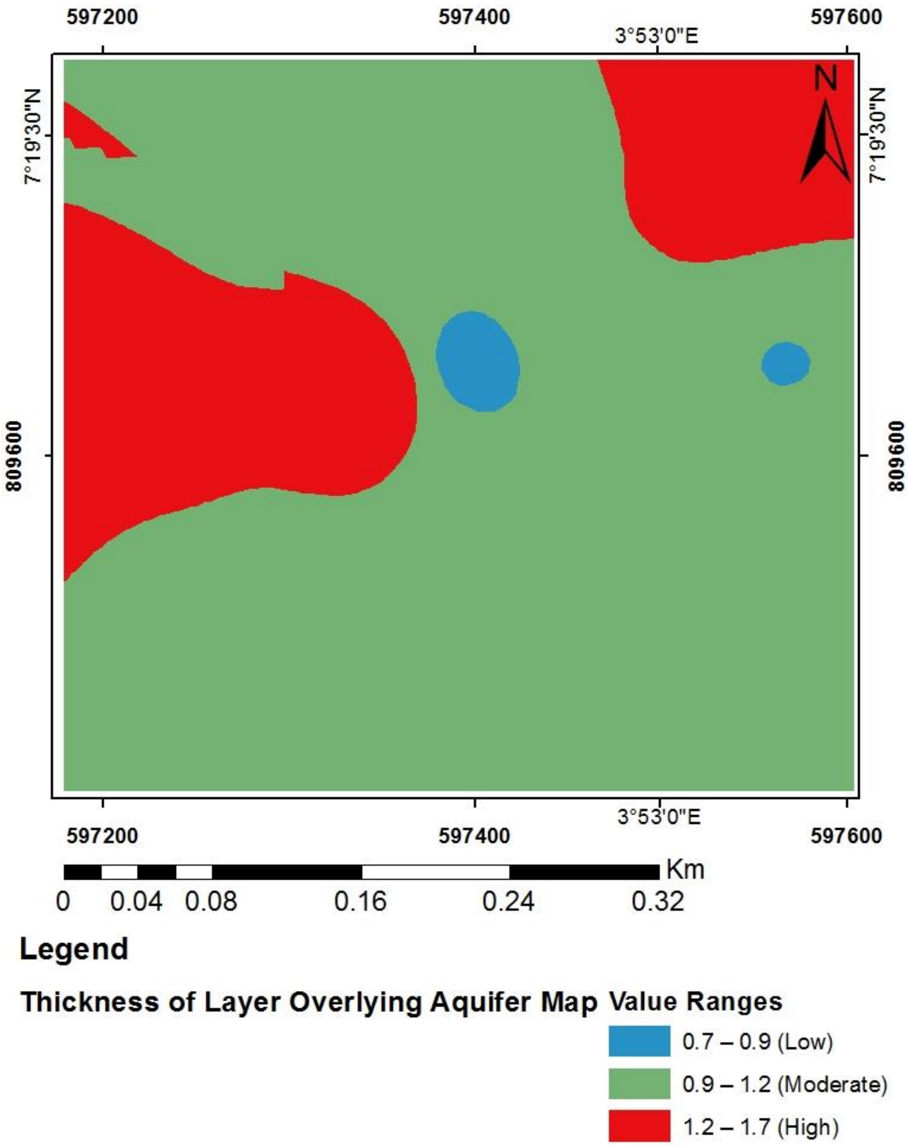

Figure 14: Thickness of Layer Overlying Aquifer Map of the Study Area

4.3.6. Hydraulic Conductivity Map of the Study Area

The hydraulic conductivity map (Figure 15) generated shows that hydraulic conductivity has values ranging from 0.00 to 0.05 hmos. A small point at the northeastern region of the investigated location is indicative of high hydraulic conductivity while northern, northeastern, northwestern, and small closure that the southeastern regions show moderate hydraulic conductivity. Low hydraulic conductivity is observed in the southern, southeastern, southwestern, and central regions of the study area which simply shows that the entire area is generally low in term of hydraulic conductivity i.e. groundwater flow.

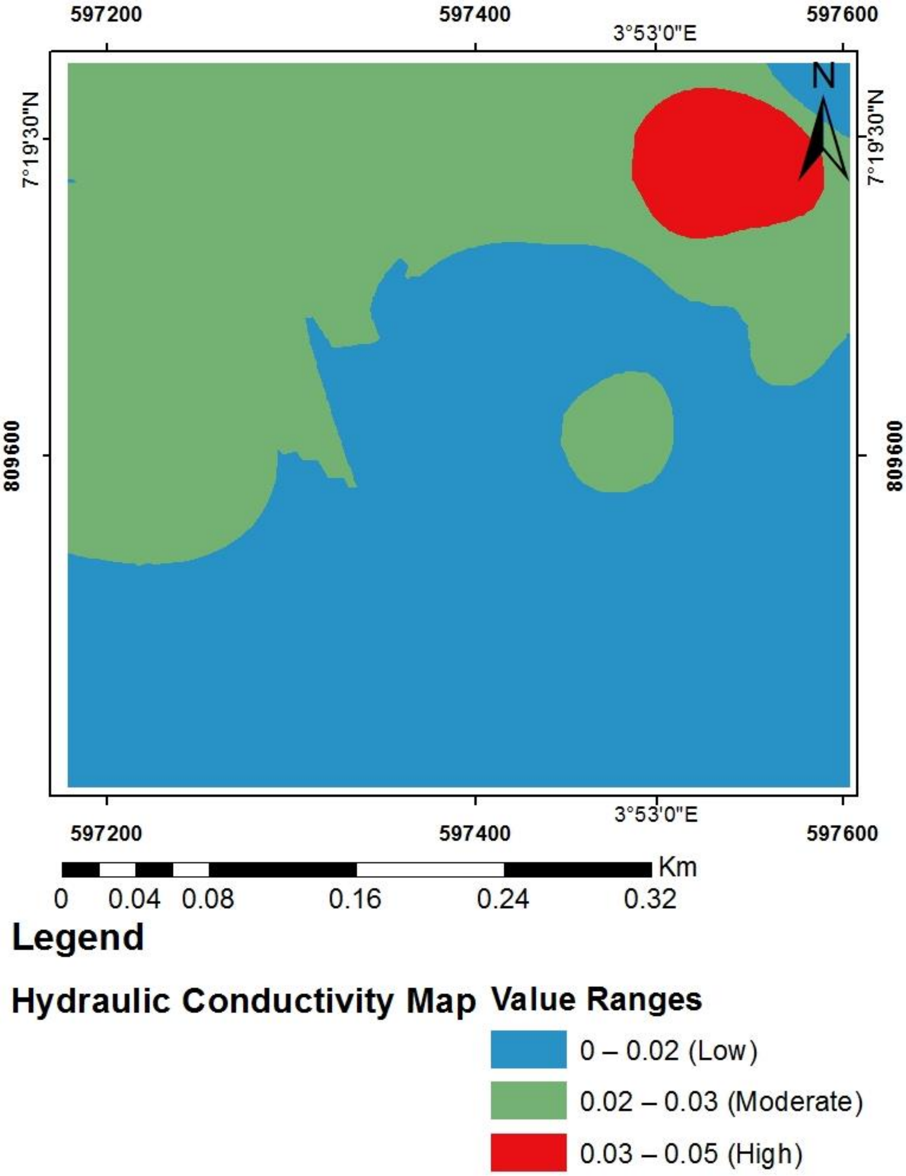

Figure 15: Hydraulic Conductivity Map of the Study Area

4.4. Dar Zarrouk Parameters for Groundwater Characteristics

The second-order parameters were used to calculate the cofficient of anisotropy with the observed value shown in Figure 18. Total longitudinal conductance value ranges from 0.004 to 0.23 Ω^{-1} within the study location (Figure 16). Total Transverse Resistance values vary from 149 to 3566 Ωm (Figure 17). While average resistivity values vary from 22.3 to 318.8 Ωm within the study location, which aids the determination of total depth (H) to the high resistivity fresh basement and average transverse resistivity values ranges from 17.6 to 807.2 Ωm. From the calculation, the coefficient of anisotropy pattern of subsurface rock formation. Th high region of coefficient of anisotropy values indicates that the fissure has given in different degrees of weathering and fracturing, which showed better water accumulation potential from diverse directions of the fissures within the rock resulting in higher porosity.

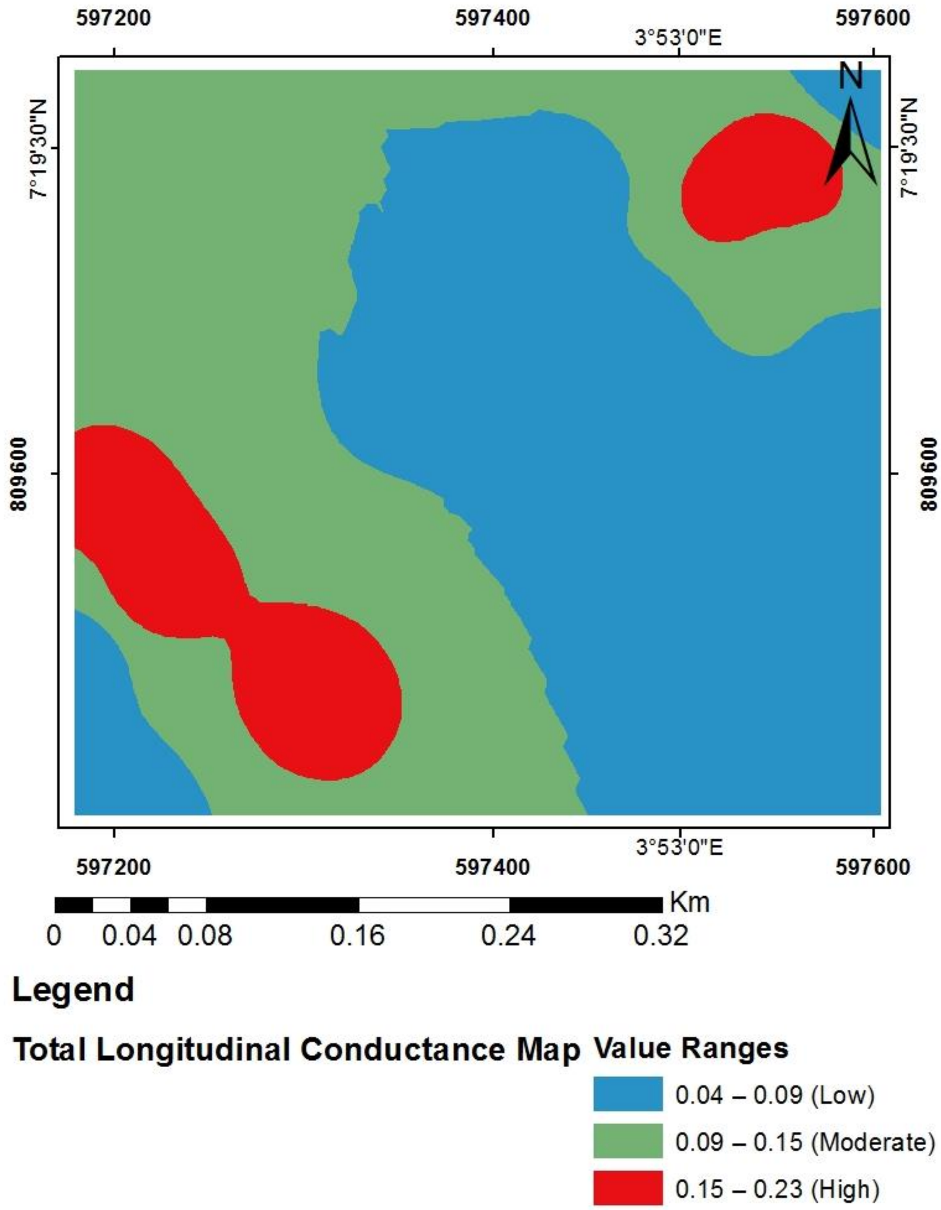

Figure 16: Total Longitudinal Conductance Map

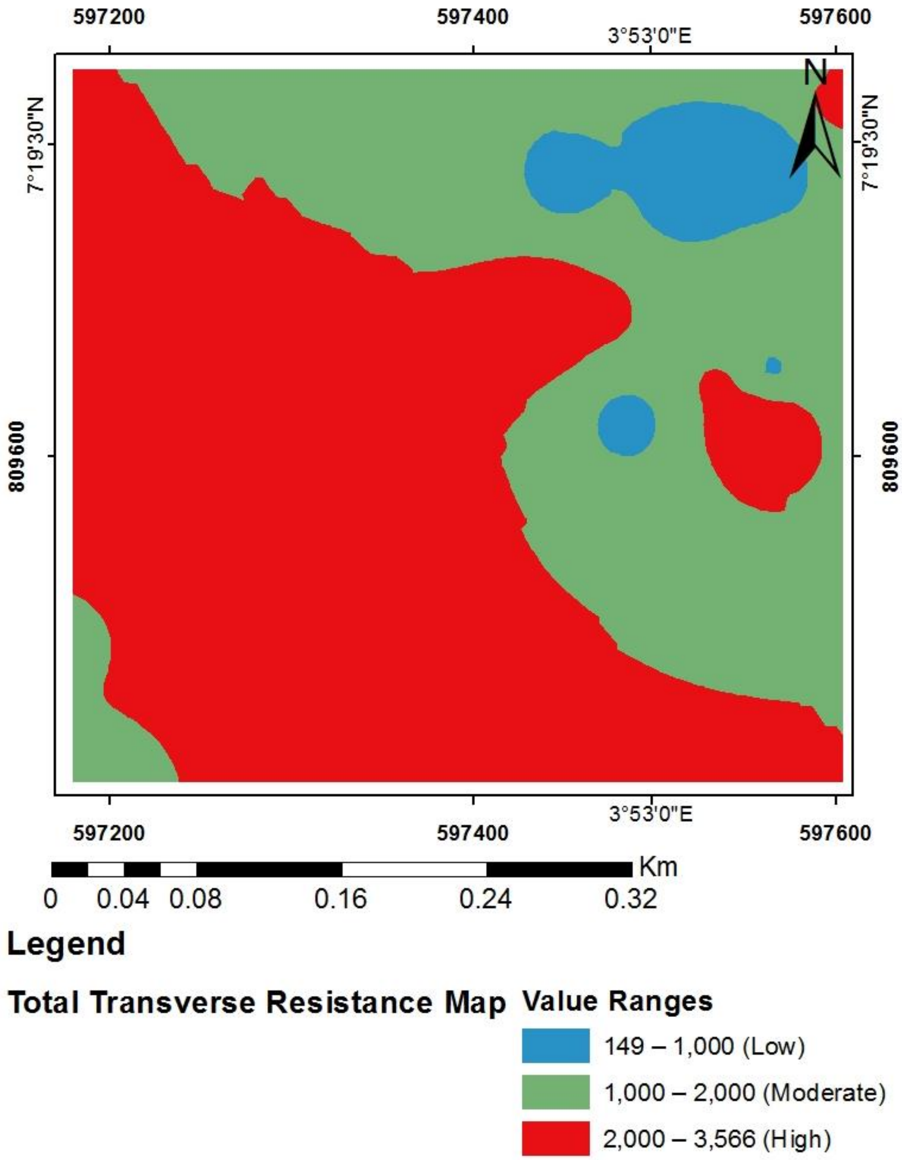

Figure 17: Total Transverse Resistance Map

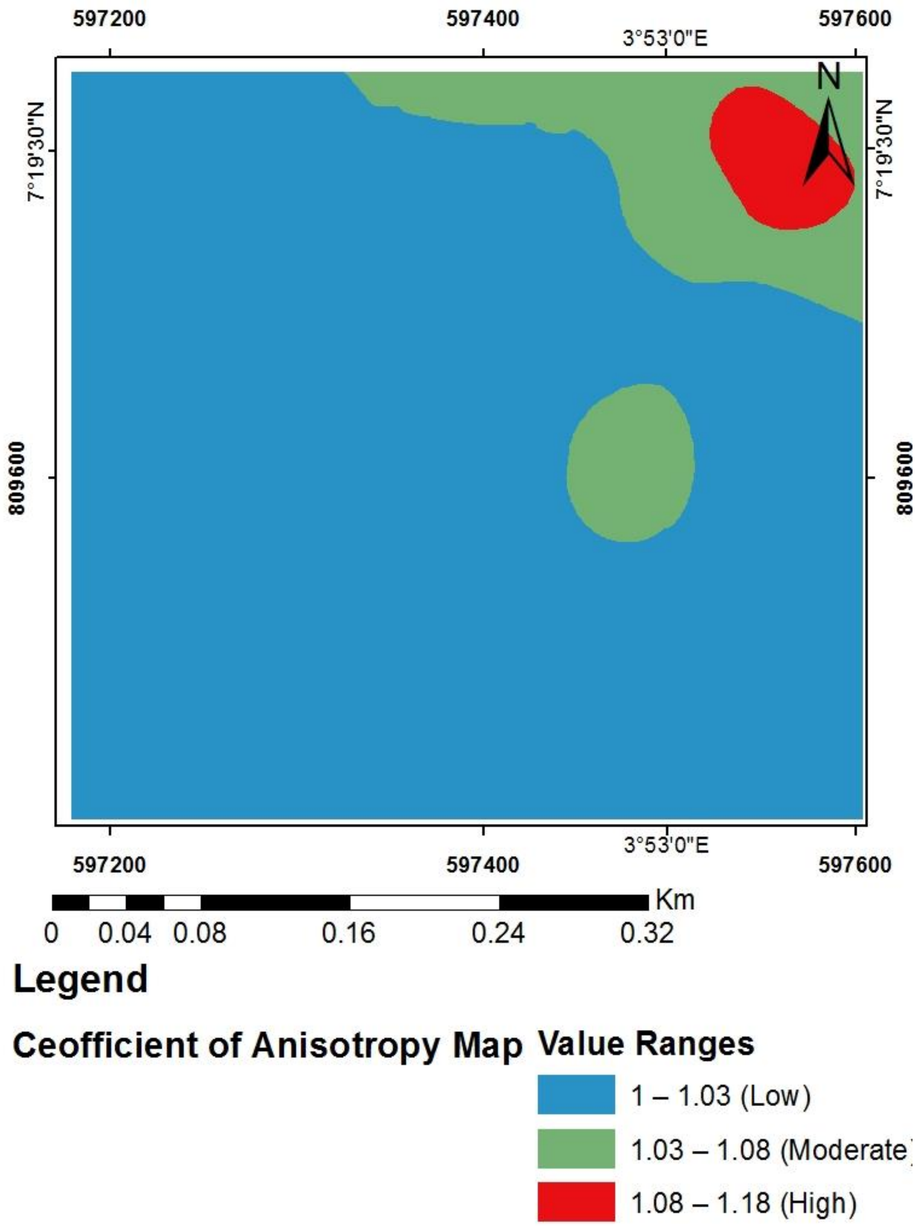

Figure 18: Coefficient of Anisotropy Map

4.5. Modeling of Aquifer Vulnerability Map

The aquifer vulnerability range determines the percentage of vulnerability prospect of different parameters. The parameters were rated and classified. Moreover, thickness and resistivity do not display the same scale, a normalized range approach was developed in categorizing these parameters regarding their significant influence on vulnerability prospect. Each parameter's type with different thickness and resistivity maps will exhibit vulnerability potential. However, each category of parameters should displayed different ratings in a range regarding its significance of storing aquifer vulnerability. Each parameter was ranged in this study in ascending order of 1-3 scale of aquifer vulnerability occurrence. The resistivity value of subsurface geologic lithologies is wide and overlaid with other subsurface fissures. Whereas, each lithology range may contain almost the same resistivity value such as longitudinal conductance, topsoil resistivity, hydraulic conductivity, and the thickness of layer overlying aquifer in the region were considered in Table 1. The weighted linear combination (WLC) was used as an equation to determine the aquifer vulnerability index (AVI)

The AVI for each parameters Oi is then determined using the equation below:

$$AVI = W_i R_i \quad (1)$$

where w_i is the weight (w) of parameter i and R_i is the rating score (R) of parameter i (Table 1)

Aquifer Vulnerability Index (AVI) of different VES points was analyzed below

$$AVI = TSR_W TSR_R + LC_W LC_R + TLOA_W TLOA_R + HC_W HC_R \quad (2)$$

The subscripts w and R indicate weights and ratings for each parameter, respectively.

Table 1: Probability rating (R) for classes of the parameters

Influencing Factors	Category (Classes)	Potentiality for Vulnerability Storage	Rating (R)	Normalized Weight (W)
Topsoil Resistivity (TSR)	61 – 150 150 – 200 200 - 317	Low Moderate High	1 2 3	0.48
Longitudinal Conductance (LC)	0.04 – 0.09 0.09 – 0.15 0.15 – 0.23	Low Moderate High	1 2 3	0.28
Thickness of Layer Overlying Aquifer (TLOA)	0.7 – 0.9 0.9 – 1.2 1.2 – 1.7	Low Moderate High	1 2 3	0.18
Hydraulic Conductivity (HC)	0.0 – 0.02 0.2 – 0.02 0.02 – 0.05	Low Moderate High	1 2 3	0.06

The aquifer vulnerability index calculated from the VES points was interpolated in ArcGIS 10.5 environment to model the aquifer vulnerability map shown in Figure 19, and the regions are categorized in table 2. A small closure in the southwestern and northeastern areas is indicative of high aquifer vulnerability zone. While northeastern, southwestern, and western regions of the investigated area show moderate aquifer vulnerability zone. The northern, southern, southeastern, southwestern, central, northeastern, and northwestern regions of the investigated area show low aquifer vulnerability zone. Also, the southwestern region of the research area is indicative of very low aquifer vulnerability zone.

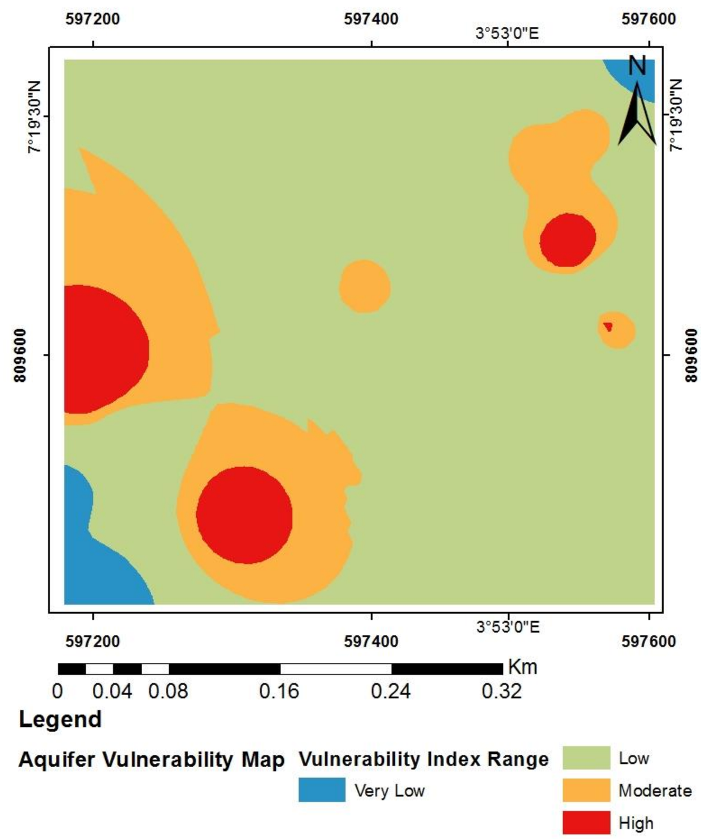

Figure 19: Aquifer Vulnerability Map of the Study Area

Table 2: Aquifer Vulnerability Classifications

Aquifer Vulnerability Values	Classifications
1.18 – 1.50	Very low
1.50 – 1.95	Low
1.95 – 2.10	Moderate
2.10 – 2.52	High

5. Conclusions

This study demonstrated the combined use of the MCDA model and GIS as an effective method for groundwater pollution vulnerability assessment. The GIS technology has provided an efficient environment for analyses and high capabilities of handling spatial data in the study area. The groundwater resources are considerably palatable in the Enterprises Hall area of Lead City University for the time being. The present study hopefully demonstrates a cost-effective method to develop improve and verify groundwater vulnerability maps. The terrain of Lead City University is generally undulating but flat in some areas. Twenty (20) Vertical Electrical Sounding points were carried out, processed, and interpreted quantitatively and qualitatively. Three subsurface geoelectric layers were delineated namely: the topsoil, weathered layer, and fresh basement. The first layer constitutes the topsoil which comprises clay, clayey sand, sandy clay, and sand with layer resistivity ranging from 62 to 226 Ωm with layer thickness varies from 0.7 to 1.7 m. The weathered layer has a resistivity value that ranges from 17 to 311 Ωm with layer thickness varying from 3.4 to 24.1 m, while the last layer is the fresh basement which is characterized by high resistivity values ranging from 429 to 2708 Ωm. The fresh basement is made up of highly resistive crystalline rock. The rocks in this region are not a water-bearing zone due to no permeability, Depth to fresh rocks ranges between 4.9 to 10.4 m. The four major parameters determined were integrated to model the aquifer vulnerability map. A small closure in the southwestern and northeastern areas is indicative of high aquifer vulnerability zone. While northeastern, southwestern, and western regions of the investigated area show moderate aquifer vulnerability zone. The northern, southern, southeastern, southwestern, central, northeastern, and northwestern regions of the investigated area show low aquifer vulnerability zone. Also, the southwestern region of the research area is indicative of very low aquifer vulnerability zone.

References

[1] S.O. Ilugbo, B.A. Adebo, K.O. Olomo, A.D. Adebiyi, “Application of GIS and multi criteria decision analysis to geoelectric parameters for modeling of groundwater potential around Ilesha, Southwestern Nigeria”, European Journal of Academic Essays, vol. 5(5), pp. 105-123, 2018a.

[2] S. O. Ilugbo, O. E. Adewoye, A. I. Aladeboyeje, U. Z. Magawata, A. A. Oyedele, T. O. Alabi, D. T. Owolabi, K. A. Adeleke, S. O. Adebayo, “Modeling of groundwater potential using remotely sensed data within Akure metropolis, Ondo State, Southwestern Nigeria”, Applied Journal of Physical Science, vol. 2(3), pp. 38-54, 2020a.

[3] M.A. Bawallah, K.A.N. Adiat, A.A. Akinlalu, S.O. Ilugbo, F.O. Akinluyi, O.O. Benjamin, A.A. Oyedele, G.O. Omosuyi, I. Aigbedion, “Groundwater Sustainability and the Divergence of Rock Types in a Typical Crystalline Basement Complex Region, Southwestern Nigeria”, Turkish Journal of Geosciences, vol. 2(1), pp. 1-11, 2021b. DOI: 10.48053/turkgeo.777217

[4] S.O. Ilugbo, A.D. Adebiyi, “Intersection of lineaments for groundwater prospect analysis using satellite remotely sensed and aeromagnetic dataset around Ibodi, Southwestern Nigeria”, International Journal of Physical Sciences, vol. 12(23), pp. 329-353, 2017.

[5] S.O. Ilugbo, H.O. Edunjobi, O.E. Adewoye, T.O. Alabi, A.I. Aladeboyeje, O.O. Olutomilola, D.T. Owolabi, “Structural Analysis Using Integrated Aeromagnetic Data and Landsat Imagery in a Basement Complex Terrain”, Southwestern Nigeria. Asian Journal of Geological Research, vol. 3(2), pp. 17-33, 2020b.

[6] B.A. Adebo, Ilugbo, S.O., Jemiriwon, E.T., Ali, A.K., Akinwumi, A.K., Adeniken, N.T. “Hydrogeophysical Investigation Using Electrical Resistivity Method within Lead City University Ibadan, Oyo State, Nigeria”, International Journal of Earth Sciences Knowledge and Applications, vol. 4(1), pp. 51-62, 2022.

[7] D. Thirumalaisan, M. Karmegam, “Aquifer vulnerability assessment using analytical hierarchy process and GIS for Upper Palar Watershed”, Center for Remote Imaging Sensing and Processing (CRISP), National University of Singapore, 2001.

[8] M.A. Bawallah, K.A.N. Adiat, A.A. Akinlalu, S.O. Ilugbo, F.O. Akinluyi, B.T. Ojo, A.A. Oyedele, O.A. Bamisaye, O.O. Olutomilola, U.Z. Magawata, “Resistivity Contrast and the Phenomenon of Geophysical Anomaly in Groundwater Exploration in A Crystalline Basement Environment, Southwestern Nigeria”, International Journal of Earth Sciences Knowledge and Applications, vol. 3(1), pp. 23-36, 2021a.

[9] A.D. Adebiyi, S.O. Ilugbo, O.E. Bamidele, T. Egunjobi, “Assessment of Aquifer Vulnerability Using Multi-Criteria Decision Analysis around Akure Industrial Estate, Akure, Southwestern Nigeria”, Journal of Engineering Research and Reports, vol. 3(3), pp. 1-13, 2018.

[10] M. Celik, “Water quality assessment and the investigation of the relationship between the River Delice and the Aquifer Systems in the vicinity of Yerköy (Yozgat)”, Environmental Geology, vol. 42, pp. 690–700, 2002.

[11] S.O. Ilugbo, H.O. Edunjobi, T.O. Alabi, A.F. Ogabi, K.O. Olomo, O.A. Ojo, K.A. Adeleke, “Evaluation of groundwater level using combined electrical resistivity log with gamma (Elgg) around Ikeja, Lagos State, Southwestern Nigeria”, Asian Journal of Geological Research, pp. 1-13, 2019.

[12] M.J. Focazio, T.E. Reilly, M.G. Rupert, D.R. Helsel, “Assessing ground-water vulnerability to contamination: providing scientifically defensible information for decision makers”, U.S. Geol. Surv. Circ., pp. 1224, 2002. Reston, Virginia.

[13] T. Harter, “Groundwater Quality and Groundwater Pollution”, Agricultural and Natural Resources (ANR), pp. 8084, 2003.

[14] Babiker, M. Mohamed, T. Hiyama, K. Kato, “A GIS based DRASTIC model for assessing aquifer vulnerability in Kakamigahara Heights, Gifu Prefecture”, Cent. Jpn. Sci. Total Environ, vol. 345, pp. 127–140, 2005.

[15] C. Simsek, C. Kincal, O. Gunduz, “A solid waste disposal site selection procedure based on groundwater vulnerability mapping”, Environmental Geology, vol. 49, pp. 620–633, 2006.

[16] S. Javadi, N. Kavehkar, K. Mohammadi, A. Khodadi, K. Kahawita, “Calibration DRASTIC using field measurements, sensitivity analysis and statistical method to assess groundwater vulnerability”, Water Int. vol. 36, pp. 719–732, 2011.

[17] N.K. Abdullahi, I.B. Osazuwa, P.O. Sule, “Application of integrated geophysical techniques in the investigation of groundwater contamination – A case study of municipal solid waste leachate”, Ozean journal of Applied Science, vol. 4, pp. 7–25, 2011.

[18] M.A. Bawallah, S.O. Ilugbo, A.O. Aina, B. Olufemi, F.O. Akinluyi, B.T. Ojo, A.A. Oyedele, N.K. Olasunkanmi, “Hydrogeophysical Studies of Central Kwara State Basement Complex of Nigeria”, International Journal of Earth Sciences Knowledge and Application, vol. 2(3), pp. 146-164, 2020b.

[19] S.O. Ilugbo, A.D. Adebiyi, K.O. Olomo, “Modeling of groundwater yield using GIS and electrical resistivity method in a basement complex Terrain, Southwestern Nigeria”, Journal of Geography, Environment and Earth Science International, vol. 16(1), pp. 117, 2018b.

[20] M.A. Bawallah, A.A. Oyedele, S.O. Ilugbo, K.O. Ozegin, B.T. Ojo, O.O. Olutomilola, E. Airewele, I. Aigbedion, “Evaluation of structural defects and the dynamic of stress and strain on a building along Oluwole Area, Southwestern Nigeria”, Applied Journal of Physical Science, vol. 2(2), pp. 23-37, 2020a.

[21] M.A. Bawallah, S.O. Ilugbo, I. Aigbedion, A.O. Aina, A.A. Oyedele, “Modeling of subsurface integrity using Dar-Zarrouk parameters: A case study of Ikekogbe UBE Primary School, Ekpoma, Edo State, Nigeria”, Journal of Geography, Environment and Earth Science International, vol. 22(1), pp. 1-17, 2019b.

[22] A.M. Bawallah, S.O. Ilugbo, B.A. Adebo, O.A. Kehinde, “Geophysical investigation for detecting buried human remains after eight years of burial in Owo, Southwestern Nigeria”, J Forensic Sci., pp. 1–9, 2021c. DOI: https://doi.org/10.1111/1556-4029.14923

[23] G.O. Omosuyi, A. Oseghale, “Groundwater vulnerability assessment in shallow aquifers using geoelectric and hydrogeologic parameters at Odigbo Res”, vol. 3(6), pp. 501-512, 2012.

[24] B.A. Adebo, E.O. Makinde, S.O. Ilugbo, “Application of Electrical Resistivity Method to Site Characterisation for Construction Purposes at Institute of Agriculture Research and Training Moor Plantation Ibadan”, Indonesian Journal of Earth Sciences, vol. 1(2), pp. 49-62, 2021.

[25] O.O. Alabi, O.O. Benjamin, M.A. Bawallah, S.O. Ilugbo, “Evaluation of Gold Mineralization Potential Using Electrical Resistivity Method Along River Chanchaga, Minna, North Central Nigeria”, International Journal of Earth Sciences Knowledge and Applications, vol. 3(3), pp. 289-300, 2021.

[26] T.A. Olla, “Integrated geophysical mapping for groundwater prospect and aquifer vulnerability around Pavillion Area, FUTA South Gate”, Nigeria. Unpl. PGD Thesis, Federal University of Technology, Akure, pp. 65-66, 2011.

[27] M.A. Bawallah, M. A. Ayuks, S. O. Ilugbo, K. O. Ozegin, A. A. Oyedele, I. Aigbedion, A. O. Aina, J. M. Whetode, K. O. Ladipo, “Geodynamics and its implications to environmental protection: A case study of Aule area, Akure, Ondo State, Southwestern, Nigeria”, Applied Journal of Physical Science, vol. 1(3), pp. 37-53, 2019a.

[28] M.A. Bawallah, A.O. Aina, S.O. Ilugbo, K.O. Ozegin, K.N. Olasunkanmi, “Evaluation of groundwater yield capacity using Dar-zarrouk parameter of central Kwara State, Southwestern Nigeria”, Asian Journal of Geological Research, pp. 1-13, 2018.

[29] S. Shahid, S.K. Nath, “GIS integration of remote sensing and electrical sounding data for hydrogeological exploration”, J Spat Hydrol, vol. 2(1), pp. 1–10, 2002.

[30] K.A.N. Adiat, M.N.M. Nawawi, K. Abdullah, “Application of Multi-Criteria Decision Analysis to Geoelectric and Geology Parameters for Spatial Prediction of Groundwater Resources Potential and Aquifer Evaluation”, Pure Appl. Geophys, vol. 170(3), 2013.

[31] B.A. Adebo, S.O. Ilugbo, E.O. Folorunsho, “Modeling of groundwater potential using Vertical Electrical Sounding (VES) and multi-caterial analysis at omitogun housing estate, Akure, southwestern Nigeria”, Asian Journal of Advanced Research and Reports, pp. 1-11, 2018.

[32] M.A. Rahaman, “Recent advances in the study of the basement complex of Nigeria. In Precambrian geology of Nigeria”, Geological survey of Nigeria, Kaduna South, pp. 11-43, 1988.

[33] C.A. Kogbe, “Preliminary study of the geology of the Nigerian sector of the Iullemmeden basin. In: Dessauvagie TFJ, Whiteman AJ (eds) African Geology”, lbadan, University Press, Nigeria, pp. 219–228, 1972.

[34] O.O. Awoniyi, “Application of geophysical investigation to evaluate the impact of a dumpsite on groundwater: Case study of Awotan-Apete, Ibadan”, Unpl. Mtech Thesis, Federal University of Technology, Akure, 2013.

[35] M.C. Cury, “Geology of degree sheet 21 (Zaria M.SC Thesis) Ahmadu Bello University”, Unpublished Thesis, 1976.